

## Article (refereed) - postprint

---

Beddows, David C.S.; Hayman, Garry D.; Harrison, Roy M.. 2012  
Enhancements to the UK Photochemical Trajectory Model for simulation of  
secondary inorganic aerosol. *Atmospheric Environment*, 57. 278-288.  
[10.1016/j.atmosenv.2012.04.020](https://doi.org/10.1016/j.atmosenv.2012.04.020)

© 2012 Elsevier Ltd.

This version available <http://nora.nerc.ac.uk/18396/>

NERC has developed NORA to enable users to access research outputs wholly or partially funded by NERC. Copyright and other rights for material on this site are retained by the rights owners. Users should read the terms and conditions of use of this material at <http://nora.nerc.ac.uk/policies.html#access>

NOTICE: this is the author's version of a work that was accepted for publication in *Atmospheric Environment*. Changes resulting from the publishing process, such as peer review, editing, corrections, structural formatting, and other quality control mechanisms may not be reflected in this document. Changes may have been made to this work since it was submitted for publication. A definitive version was subsequently published in *Atmospheric Environment*, 57. 278-288. [10.1016/j.atmosenv.2012.04.020](https://doi.org/10.1016/j.atmosenv.2012.04.020).

[www.elsevier.com/](http://www.elsevier.com/)

Contact CEH NORA team at  
[noraceh@ceh.ac.uk](mailto:noraceh@ceh.ac.uk)

1  
2  
3  
4  
5  
6  
7  
8  
9  
10  
11  
12  
13  
14  
15  
16  
17  
18  
19  
20  
21  
22  
23  
24  
25

# ENHANCEMENTS TO THE UK PHOTOCHEMICAL TRAJECTORY MODEL FOR SIMULATION OF SECONDARY INORGANIC AEROSOL

DAVID C. S. BEDDOWS<sup>1</sup>, GARRY HAYMAN<sup>2</sup>  
AND ROY M. HARRISON<sup>1,1\* †</sup>

<sup>1</sup> National Centre for Atmospheric Science  
School of Geography, Earth & Environmental Sciences  
Division of Environmental Health & Risk Management  
University of Birmingham, Edgbaston  
Birmingham, B15 2TT, United Kingdom

<sup>2</sup> Centre for Ecology and Hydrology  
Maclean Building, Benson Lane  
Crowmarsh Gifford, Wallingford  
Oxfordshire, OX10 8BB, United Kingdom

---

\* To whom correspondence should be addressed (Tel: +44 121 414 3494; Fax: +44 121 414 3709;  
Email: [r.m.harrison@bham.ac.uk](mailto:r.m.harrison@bham.ac.uk))

†Also at: Department of Environmental Sciences / Center of Excellence in Environmental Studies, King Abdulaziz University, Jeddah, 21589, Saudi Arabia

## 26 **Abstract**

27 Particulate matter remains a challenging pollutant for air pollution control in the UK  
28 and across much of Europe. Particulate matter is a complex mixture of which secondary  
29 inorganic compounds (sulphates, nitrates) are a major component. This paper is  
30 concerned with taking a basic version of the UK Photochemical Trajectory Model and  
31 enhancing a number of features in the model in order to better represent boundary layer  
32 processes and to improve the description of secondary inorganic aerosol formation. The  
33 enhancements include an improved treatment of the boundary layer, deposition processes  
34 (both wet and dry), attenuation of photolysis rates by cloud cover, and inclusion of the  
35 aerosol thermodynamic model ISORROPIA II to account both for chemistry within the  
36 aerosol and between the particles and gas phase. Emissions inventories have been  
37 updated and are adjusted according to season, day of the week and hour of the day.  
38 Stack emissions from high level sources are now adjusted according to the height of the  
39 boundary layer and a scheme for generating marine aerosol has been included. The skill  
40 of the improved model has been evaluated through predictions of the concentrations of  
41 particulate chloride, nitrate and sulphate and the results show increased accuracy and  
42 lower mean bias. There is a much higher proportion of the values lying within a factor of 2  
43 of the observed values compared to the basic model and Normalised Mean Bias has  
44 reduced by at least 89% for nitrate and sulphate. Similarly, the Index of Agreement  
45 between calculated and measured values has improved by ~10%. Considering the  
46 contribution of each enhancement to the improvement in the performance metrics, the  
47 most significant enhancement was the replacement of the parameterisation of the  
48 boundary layer height, relative humidity and temperature by HYSPLIT values calculated  
49 for each trajectory. The second most significant enhancement was the parameterisation of  
50 the photolysis rates by values calculated by an off line database accounting for the  
51 dependence of photolysis rates on zenith angle, cloud cover, land surface type and column  
52 ozone. The inclusion of initial conditions which were dependent on the starting point of the  
53 trajectory and the modulation of stack emissions made the most significant improvement to  
54 sulphate. Furthermore, in order to assess the model's response to abatement scenarios,  
55 30% abatements of either NH<sub>3</sub>, NO<sub>x</sub> or SO<sub>2</sub> showed a reduction in the sum of chloride,  
56 nitrate and sulphate of between 3.1 % to 8.5 % (with a corresponding estimated reduction  
57 of 1.6 – 3.7% reduction in PM<sub>10</sub>). The largest reduction in this contribution is due to the  
58 abatement of NO<sub>x</sub>.

59 **Keywords:** Lagrangian model; sulphate; nitrate; chloride; Master Chemical Mechanism

## 60 Introduction

61 The United Kingdom, along with other European countries, is required to meet  
62 stringent air quality standards for PM<sub>10</sub> and PM<sub>2.5</sub>, as well as exposure reduction targets  
63 for PM<sub>2.5</sub> set by the European Union (EC, 2008). Abatement strategies to improve air  
64 quality with respect to particulate matter (PM) pollution have considerable economic cost.  
65 The Directive on “Ambient Air Quality and Cleaner Air for Europe” for example estimates  
66 the cost of the ‘Maximum Technically Feasible Reduction’ scenario, abating SO<sub>2</sub>, NO<sub>x</sub>,  
67 VOC, NH<sub>3</sub>, and PM<sub>2.5</sub>, to be € 39.7 billion per year in the year 2020. Additional measures  
68 may be needed as there has been little change in annual mean concentrations of PM<sub>10</sub>  
69 since the year 2000 across considerable parts of Europe (Harrison et al., 2008, UN ECE  
70 report on PM, 2007: <http://tarantula.nilu.no/projects/cccr/reports/cccr8-2007.pdf>).

71 Airborne particulate matter, be it expressed as PM<sub>2.5</sub> or PM<sub>10</sub> mass, is a complex  
72 mixture of chemical constituents. In the UK, the predominant individual constituents are  
73 sulphates, nitrates and organic matter. Campaign data was collected in the months of May  
74 and November of the years 2004 and 2005, in central Birmingham (Yin and Harrison,  
75 2008), showing that sulphates and nitrates account on average for 34.5% of PM<sub>10</sub> and  
76 45.2% of PM<sub>2.5</sub> mass with the rest comprising of organics (PM<sub>10</sub>; PM<sub>2.5</sub> = 23.7%; 26.1%),  
77 iron rich dust (PM<sub>10</sub>; PM<sub>2.5</sub> = 13.4%; 5.9%), elemental carbon (PM<sub>10</sub>; PM<sub>2.5</sub> = 8%; 11.2%),  
78 sodium chloride (PM<sub>10</sub>; PM<sub>2.5</sub> = 9.3; 4%) and calcium salts (PM<sub>10</sub>; PM<sub>2.5</sub> = 7.4%; 2.5%).  
79 During episodes of elevated PM concentrations exceeding the daily European Limit Value  
80 of 50 µg m<sup>-3</sup>, the contribution of sulphates and nitrates increased to 57.2% of PM<sub>10</sub> and  
81 68.5% of PM<sub>2.5</sub> (Yin and Harrison, 2008) and were associated with transport of secondary  
82 pollutants. Consequently, abatement of these components is potentially an attractive  
83 policy option focussing on their precursor gases emitted by traffic, industry and domestic  
84 sources (Erisman and Schaap, 2004, AQEG, 2005, Jones and Harrison, 2011).

85 Numerical models have an important part to play in predicting the impact of  
86 abatement strategies and a number of such models have been used to predict  
87 concentrations of particulate matter components within the European atmosphere. These  
88 include Eulerian models such as LOTOS-EUROS (Schaap et al., 2008), CHIMERE  
89 (Bessagnet et al., 2009), REM-CALGRID model (RCG) (Beekmann et al., 2007), and the  
90 Unified EMEP model (Simpson et al. 2011) to name but a few. The unified EMEP model  
91 has been used for policy development in Europe (Aas et al., 2007) to address regional  
92 scale impacts of NO<sub>x</sub> and SO<sub>2</sub> emission reductions on PM mass concentrations (despite  
93 having uncertainties of about ± 40% for nitrate).

94 In the UK, the Photochemical Trajectory Model (PTM) has often been used to  
95 understand boundary-layer pollution. For example, Walker et al. (2009) and Baker (2010)  
96 simulated concentrations of ozone, and Derwent et al. (2009b) modelled concentrations of  
97 sulphate and nitrate. The PTM is a boundary-layer Lagrangian model whose main  
98 advantage over the Eulerian modelling approach is its ability to run highly comprehensive  
99 chemical schemes without simplifications and parameterisations that may compromise the  
100 performance of the chemical reaction scheme. The PTM is therefore suited to the  
101 examination of abatement policies aimed at targeting emissions of individual precursors  
102 (e.g. NH<sub>3</sub>, NO<sub>x</sub>, SO<sub>2</sub>). A number of studies have modelled particulate matter in Europe.  
103 Most notably, the CityDelta project compared the ability of several models to predict the  
104 impact of emissions reductions upon concentrations in European cities (Cuvelier et al.,  
105 2007), specifically Berlin, Milan, Paris and Prague (Thunis et al., 2007). A subsequent  
106 study (Stern et al., 2008) examined the ability of five chemical transport models to  
107 reproduce PM<sub>10</sub> episode conditions in central Europe. Model specific studies, such as  
108 those with CHIMERE, have sought to simulate particulate matter concentrations in specific  
109 parts of Europe, e.g. Portugal (Monteiro et al., 2007) and northern Italy (de Meij et al.,  
110 2009). Air quality models used for calculating aerosol species over the UK include the  
111 Community Multiscale Air Quality model (CMAQ), Chemel et al., 2010) and the Hull Acid  
112 Rain Model (HARM), (Metcalf et al., 2005). CMAQ over-predicted O<sub>3</sub> and under-  
113 predicted aerosol species with the exception of sulphate (Chemel et al., 2010). The  
114 HARM and ELMO models (Whyatt et al., 2007) underestimated sulphate, nitrate and  
115 ammonium by a large margin, and chloride massively. In the work of Redington and  
116 Derwent (2002), the NAME model slightly under-predicted measured sulphate values  
117 although the annual average values of nitrate compared well.

118 We have previously used the UK Photochemical Trajectory Model (a version of the  
119 Derwent et al. (2009b) UK-PTM) to model concentrations of particulate sulphate and  
120 nitrate in southern England and Northern Ireland in 2002 (Abdalmogith et al., 2006). While  
121 our study was quite successful in modelling monthly mean concentrations and trends in  
122 both nitrate and sulphate, it performed poorly in modelling daily concentration data,  
123 especially during nitrate and sulphate episodes which were observed during easterly  
124 transport trajectory events that brought high levels of particulate matter from Europe. It  
125 was concluded that this was unlikely to be due to errors in the back trajectory alone and  
126 that inclusion of a more sophisticated treatment of emissions and meteorology would  
127 probably be required to address the issue adequately. It was also recognised that it would  
128 be advantageous to: (i) use more than one photochemical back trajectory calculation for

129 each daily measurement, (ii) update emissions inventories and injection parameters to  
130 account for daily and seasonal variation; (ii) add wet deposition processes; (iii) replace the  
131 dynamic approach which treated the chemistry of the  $\text{NH}_4\text{NO}_3$  –  $\text{HNO}_3$  –  $\text{NH}_3$  system as a  
132 bimolecular gas phase reaction with a more sophisticated thermodynamic algorithm,  
133 ISORROPIA II and (iii) and replace the clear-sky photolysis rates with ones which  
134 accounted for cloud cover.

135 Numerous amendments have been applied to the original model to form an  
136 enhanced UK-PTM with a view to providing an improved model aimed at addressing  
137 policymaking decisions. In this paper, we assess the changes resulting from the  
138 enhancements by using observed gas- and aerosol-phase data collected at the Harwell  
139 observatory in Oxfordshire, UK in 2007.

140

## 141 **TECHNICAL DESCRIPTION OF THE MODIFICATIONS TO THE UK-PTM**

142 The UK-PTM is a boundary-layer trajectory model originally assembled to simulate  
143 photochemical ozone production and subsequently used to derive Photochemical Ozone  
144 Creation Potentials (POCPs) (Derwent et al., 1998, Derwent et al., 2005). The model was  
145 initially set up to represent an idealised summertime photochemical episode occurring over  
146 the UK and used linear air mass trajectories. More recent studies have used air mass  
147 back trajectories calculated from meteorological wind velocity vector fields and a  
148 parameterised boundary layer height (Abdalmogith et al., 2006; Derwent et al., 2009b;  
149 Walker et al., 2009 and Baker, 2010). The changes made by these authors have  
150 improved the PTM. Here, we have modified the PTM further to include a new treatment of  
151 aerosol processes and of emissions from tall stacks, the effect of cloud cover on photolysis  
152 values, wet deposition, and a revised treatment of the emissions, amongst others. A  
153 complete list of changes made to the emissions inventories, chemical mechanism and  
154 back trajectory calculation is presented in Table 1.

155

### 156 **Initial Conditions**

157 An implicit assumption made in the original model (Abdalmogith et al., 2006) was that  
158 all trajectories, if they were extrapolated far enough back in time, would start over the  
159 Atlantic. The initial conditions were fixed to one set of values derived from a remote  
160 marine location off the west coast of the Republic of Ireland. In practice, 3-5 day back  
161 trajectories with arrival points in the UK do not all start over the Atlantic but may start over  
162 continental Europe. Stohl (1998) recommends that these trajectories are not further  
163 lengthened in order to maintain a reasonable level of certainty of their position. The

164 amended model uses 5 starting regions, namely Western, Northern, Eastern, Southern  
165 and Central (Figure 1) to which initial concentrations of HCl, NO, NO<sub>2</sub>, NO<sub>3</sub>, HNO<sub>3</sub>, SO<sub>2</sub>,  
166 SO<sub>4</sub>, CO, CO<sub>2</sub>, CH<sub>4</sub>, HCHO, O<sub>3</sub>, NH<sub>3</sub>, NH<sub>4</sub><sup>+</sup>, NO<sub>3</sub><sup>-</sup> and SO<sub>4</sub><sup>2-</sup> were assigned (see Table S1  
167 in Supplementary Information). These initial concentrations were derived from data  
168 measured at Birkenes, Braganca, Campisabolos, Glashaboy, Hohenpeissenberg, Ispra,  
169 Melpitz, Montelibretti, Norway Ocean Station, and S. Pietro Capofiume between 2000 and  
170 2007. The initial concentrations were averaged over the measurements taken at a site  
171 which best represented the conditions within the initial zone, e.g. for the Western or  
172 Northern initial conditions, the most representative measurements are those collected at  
173 Birkenes with back-trajectories crossing only over the ocean or the polar ice cap. There is  
174 scope in the future to increase the number of starting zones and to make seasonal  
175 adjustments to these values or to use concentration fields provided from larger domain  
176 models.

177

## 178 **Meteorology**

179 The majority of studies use back trajectories with a timescale of 3-5 days. This is  
180 generally a compromise between having sufficient time to describe the long-range  
181 transport and the decreasing accuracy of individual back trajectories the further they are  
182 projected backward in time (Stohl, 1998). In this work, four-day back trajectories were  
183 calculated using the NOAA Hybrid Single Particle Lagrangian Integrated Trajectory  
184 (HYSPLIT-4) model (Draxler and Hess, 1998) and the archived NCEP/NCAR global data  
185 assimilation system data (GDAS). The original UK PTM was simply based on three day  
186 ECMWF back trajectories consisting of latitude/longitude values calculated online by  
187 BADC.

188 An improvement in accuracy can also be achieved by averaging over the values  
189 obtained from the output of more than one photochemical back trajectory for each daily  
190 PM measurement. Instead of using a single trajectory with a specific arrival time e.g.  
191 during the mid-afternoon at 15:00 h (as in the case of Baker (2010) who considered air  
192 parcel trajectories arriving in Birmingham, UK), our model was adapted to run  
193 photochemical calculations along trajectories for air masses arriving every hour of the day.  
194 This implied that for each daily PM<sub>10</sub> filter measurement, an average calculated value was  
195 determined based on meteorological conditions which were liable to change significantly  
196 over the course of a day. Other multiple trajectory sampling schemes can potentially use  
197 trajectories arriving at different heights and/or at many nodes of a gridded zone placed  
198 symmetrically around the receptor site (private communication with R. Derwent, 2008).

199 In addition to latitude and longitude, other parameters are included in the back  
200 trajectory data, namely the boundary layer height, relative humidity and temperature. The  
201 HYSPLIT boundary layer heights give a more realistic description of the boundary-layer  
202 (BL) and replace the “clipped saw-tooth” function used in the earlier model of Abdalmogith  
203 et al. (2006) and shown in Figure S4 which is based on an idealised summertime episode.  
204 In particular, in HYSPLIT, the height of the mixing layer is taken as the height at which the  
205 potential temperature is at least two degrees greater than the minimum potential  
206 temperature. When plotted, the temporal boundary layer height profiles are no longer  
207 angular, they change more progressively and they are correctly synchronised to the rising  
208 and falling of the sun no matter at what latitude the air mass is located at. As the boundary  
209 layer expands, the constituents in the supra layer are mixed into the boundary layer and at  
210 dusk the supra layer concentrations are made equal to the boundary layer concentrations  
211 at dusk. However, as the boundary layer depth decreases, the constituents in the  
212 boundary layer are mixed back into the supra layer. There is no chemical evolution of the  
213 upper box.

214 Further auxiliary values in the back trajectory data included the 10 m wind velocity  
215  $U_{10}$  and hourly rain rates  $f$  which were inputted into the parameterisation of sea salt flux  
216 and PM deposition respectively. Cloud cover and time/date data are also included so that  
217 the clear-sky assumption could be removed from the model and the emission flux  
218 corrections could be correctly synchronised to the hour of the day, day of the week and  
219 month of the year.

220

## 221 **Chemistry**

222 In order to include a more sophisticated treatment of aerosol properties (e.g.  
223 inclusion of ISORROPIA II) and to speed up the calculation, the Master Chemical  
224 Mechanism (MCM 3.1) was replaced with the Common Reactive Intermediate (CRI)  
225 mechanism (version CRI v02) developed by Jenkin et al. (2008). Jenkin et al. (2008) have  
226 shown that the CRI mechanism is virtually equivalent to the full MCM. This reduction in  
227 the number of species and reactions reduced the calculation time for one trajectory from  
228 one hour to approximately one minute. Watson et al. (2008) have made further reductions  
229 in the CRI mechanism by removing specific VOCs and reallocating the emissions to  
230 retained VOCs, but these reduced mechanisms were not included.

231 The VOC speciation used in this study is based on the speciated VOC emission  
232 inventory for 2000 compiled by Passant (2002) as part of the UK National Atmospheric  
233 Emission Inventory (NAEI) programme for the 2002 inventory year (the latest available at

234 the time of the original model development). This speciated emission inventory comprised  
235 664 VOCs emitted from 249 source sectors with a total annual emission of 1543.7  
236 ktonnes, including natural VOC emissions of 178 ktonnes per annum. The emissions from  
237 the 249 source sectors were aggregated to the relevant SNAP-1 sector. As many of the  
238 VOCs in the UK inventory were isomers or related to the model VOCs, the assignments  
239 were relatively straightforward.

240 In the original model, a clear sky scenario was always in place generally limiting the  
241 application of the model to summer conditions. The photolysis values  $J$  were  
242 parameterised to the solar zenith angle  $Z$ , using equation 1, where  $l$ ,  $m$ ,  $n$ , are constants  
243 available from the MCM website (<http://mcm.leeds.ac.uk/MCM>).

$$J = l(\cos Z)^m \exp(-n \sec Z) \quad (1)$$

244 In the enhancement, the photodissociation rates were calculated off line using the  
245 PHOTOL code (Hough, 1988). This has been updated to account for changes to  
246 spectroscopic and photochemical parameters, most notably the quantum yield of ozone  
247 (Atkinson et al., 1997). The input database contains the dependence of photolysis rates  
248 for 21 species on zenith angle, cloud cover, land surface type and column ozone. The  
249 local photolysis rates were derived during the model run by identifying the nearest element  
250 in the database. The aerosol and ozone columns were initially fixed, the latter at ~300 DU,  
251 but could be varied subsequently. The tabular values not only accounted for the solar  
252 zenith angle at a given time of the day, latitude and longitude, but also account for the  
253 surface over which the air mass travels (surface albedo of land, sea or ice) and the  
254 fractional cloud cover which was included as a field within the back trajectory data.  
255 Fractional cloud cover values were extracted, for each step of the trajectory, from Global  
256 Data Assimilation System (GDAS) forecast data generated by the National Weather  
257 Service's National Centers for Environmental Prediction (NCEP)  
258 (<http://ready.arl.noaa.gov/gdas1.php>). Using this system, values of photosynthetically  
259 active radiation (PAR) are also derived for the calculation of an environmental correction  
260 factor for monoterpenes and isoprenes calculated in the biogenic emission inventories  
261 (Figure S5).

262

## 263 **Aerosol Processes**

264 In the original UK-PTM, the aerosol chemistry was accounted for by a very simple  
265 process to represent the establishment of thermodynamic equilibrium in the  $\text{NH}_4\text{NO}_3$  –  
266  $\text{HNO}_3$  –  $\text{NH}_3$  system. Ammonia was rapidly combined with available aerosol sulphate to

267 form ammonium sulphate and any ammonia that remained was assumed to form a  
 268 thermodynamic equilibrium with nitric acid and ammonium nitrate. No account was taken  
 269 of hygroscopic water uptake which substantially affects the equilibrium. Furthermore, the  
 270 formation of coarse mode aerosol nitrate was parameterised by the reaction of N<sub>2</sub>O<sub>5</sub> and  
 271 nitric acid with natural dusts and sea salt. Abdalmogith et al. (2006) and Derwent et al.  
 272 (2009b) provide more details. The parameterisations based on the concentrations of the  
 273 trace gases NH<sub>3</sub>, N<sub>2</sub>O<sub>5</sub>, HNO<sub>3</sub>, and SO<sub>3</sub> have been replaced in the enhanced model by the  
 274 aerosol thermodynamic equilibrium model for K<sup>+</sup>, Ca<sup>2+</sup>, Mg<sup>2+</sup>, NH<sub>4</sub><sup>+</sup>, Na<sup>+</sup>, SO<sub>4</sub><sup>2-</sup>, NO<sub>3</sub><sup>-</sup>, Cl<sup>-</sup>,  
 275 H<sub>2</sub>O aerosols and associated gases, called ISORROPIA II (Fountoukis et al., 2009). In  
 276 this work, it was compiled from FORTRAN code into a dynamic link library accessible by  
 277 the FACSIMILE model. The complete theory of ISORROPIA II, together with a detailed  
 278 description of the equations solved, the activity coefficient calculation methods and the  
 279 computational algorithms used can be found in Nenes et al. (1998a,b) and Fountoukis and  
 280 Nenes (2007).

281

## 282 **Aqueous Phase Processes**

283 The aqueous phase oxidation of SO<sub>2</sub> to H<sub>2</sub>SO<sub>4</sub> in clouds is treated using a pseudo  
 284 first-order process with a reaction constant R<sub>k</sub>. The original value for R<sub>k</sub> based on an  
 285 assumed conversion of 1-2% / hour was replaced by a parameterisation based on relative  
 286 humidity and cloud cover ε, (see equation 2 and Schaap et al. (2004)).

$$R_k = \begin{cases} 5.8 \times 10^{-5}(1 + 2\varepsilon), & RH < 90 \% \\ 5.8 \times 10^{-5}(1 + 2\varepsilon)[1.0 + 0.1 * (RH - 90.0)], & RH \geq 90 \% \end{cases} \quad (2)$$

287

## 288 **Deposition Values**

289 The conventional resistance approach - reviewed by Wesely and Hicks (2000) - of  
 290 representing dry deposition processes was used in the model. The rate of dry deposition  
 291 of the chemical species *i*, of concentration C<sub>*i*</sub>, was given by,

$$\frac{d}{dt}[C_i] = -\frac{v_g}{H}[C_i] \quad (3)$$

292 where the boundary layer height and deposition velocity are represented by *H* and *v<sub>g</sub>*  
 293 respectively. For gases, tabulated dry deposition values were subdivided in the model to  
 294 account for whether the air mass was over land or sea (see Table S2). For ozone, a  
 295 more developed representation was used which accounted for the diurnal and seasonal  
 296 variation induced by stomatal opening and closing. In the model, the approximation of the  
 297 half sinusoidal function described by Hayman et al. (2010) was used. Further

298 improvements could be made by accounting for the opening and closing of stomata in  
 299 response to the availability of moisture and the meteorological conditions. This adjusts the  
 300 deposition value of ozone between a night time and winter constant value of  $2 \text{ mm s}^{-1}$  and  
 301 a seasonal maximum ranging from 4 to  $7 \text{ mm s}^{-1}$  (Hayman, 2010).

302 For particulate matter (in this case for chloride, nitrate and sulphate particles) dry-  
 303 deposition was accounted for by an expression developed by Smith et al. (1993) primarily  
 304 for air masses as they move over the sea (equation 4),

$$V_d = \frac{V_t}{1 - \exp\left\{-\left(\frac{V_t}{CD \cdot U_{10}}\right)\right\}} \quad (4)$$

305 This is a function of the 10 m wind speed  $U_{10}$ , the gravitational sedimentation velocity  
 306  $V_t$  and the Drag Coefficient  $CD$ , between the atmosphere and ocean (equation 5).

$$CD(U_{10}) = \begin{cases} 1.14 \times 10^{-3}, & U_{10} \leq 10 \text{ ms}^{-1} \\ (0.49 + 0.065U_{10}) \times 10^{-3}, & U_{10} > 10 \text{ ms}^{-1} \end{cases} \quad (5)$$

307 This expression (eq. 4) was used for land multiplied by a ratio of typical fixed  
 308 land/sea values for  $1 \mu\text{m}$  particles.

309 An additional loss term  $\Lambda_g$ , was added to represent removal by wet deposition using  
 310 the parameterisation given by McMahon et al. (1979). This is a function of hourly rainfall  $f$   
 311 which was taken from the HYSPLIT back trajectory data (equation 6). The expression for  
 312  $\text{SO}_2$  appears in equation 6, where  $f$  is the rainfall rate ( $\text{mm h}^{-1}$ )

$$\Lambda_g = 17 \times 10^{-5} f^{0.6} \quad (6)$$

313

## 314 **Emission Inventories**

315 Emission fluxes were calculated using one of two sets of  $\text{SO}_2$ ,  $\text{NO}_x$ , NMVOC, CO and  
 316  $\text{NH}_3$  emission inventories. For the UK land mass, NAEI emission data were used  
 317 (<http://naei.defra.gov.uk/>). The NAEI inventory programme produces annual emission  
 318 maps at  $1 \text{ km} \times 1 \text{ km}$  spatial resolution for the major emission source sectors. These were  
 319 aggregated to  $10 \text{ km} \times 10 \text{ km}$  for each pollutant and major source sector. Emission data  
 320 were taken from EMEP (<http://www.emep.int/>) for the remaining model domain. These  
 321 were available on a  $50 \text{ km} \times 50 \text{ km}$  grid for the same pollutants and major emission source  
 322 sectors. The base year for the emissions was 2005 (the latest available at the time of the  
 323 work), which were scaled to 2007 using the ratio of the national sector emission totals for  
 324 2005 and 2007 for each country. In a similar manner to that adopted by Hayman et al.  
 325 (2010), a separate term was added to represent the emissions of VOCs from natural  
 326 sources (taken to be trees), This is described further below.

327

328 *Emission fluxes*

329 Instantaneous emission fluxes were derived from the annual average emission  
330 inventories for SO<sub>2</sub>, NO<sub>x</sub>, CO, NH<sub>3</sub>, VOCs and NMVOCs and updated every 30 minute  
331 trajectory step within the calculation as the air mass moved across the model domain. The  
332 emissions were calculated from the annual emissions of NH<sub>3</sub>, NO<sub>x</sub>, VOCs, biogenic VOCs,  
333 EC, and OC, scaled by factors describing diurnal, day-of-week, and monthly variations  
334 which were published as part of the City-Delta European Modelling Exercise  
335 ([http://aqm.jrc.ec.europa.eu/citydelta/temp\\_factors\\_gh.txt](http://aqm.jrc.ec.europa.eu/citydelta/temp_factors_gh.txt))

336 *Biogenic emission fluxes*

337 Additional emission terms are added to the emission rate of isoprene and terpenes to  
338 represent the natural biogenic emissions from European forests and agricultural crops.  
339 The emission inventory used was that derived in the PELCOM project (PELCOM, 2000).  
340 The inventory was aggregated to the EMEP 50 km x 50 km grid and gives emission  
341 potentials for isoprene (from deciduous and evergreen trees: temperature and light-  
342 sensitive), monoterpenes (from deciduous and evergreen trees: temperature or  
343 temperature and light-sensitive) and other VOCs (OVOCs, from deciduous and evergreen  
344 trees: temperature sensitive). The emission potentials were converted to local emission  
345 rates using environmental correction factors (Guenther, 1997), derived from the  
346 meteorological datasets. Hayman et al. (2010) compared the PELCOM emission  
347 inventory with other estimates and discussed the implications of using this inventory.

349 *Sea salt emission flux*

350 In order to use ISORROPIA II, a sodium and chloride concentration were required  
351 and this was derived from a sea-salt parameterisation developed by Gong (2003). Figure  
352 S1 shows the flux distribution (equation 7) used to derive an injection term in the model  
353 which was dependent on the wind speed at 10 m (U<sub>10</sub>). This term was integrated into a  
354 mass flux (using particle density to mass density relationship,  $\frac{dm}{dr} = m_p \frac{dF}{dr}$ ) for all particle  
355 radii r, reducing the parameterisation to a term involving just U<sub>10</sub>,

$$\frac{dF}{dr} = 1.373u_{10}r^{-A}(1 + 0.057r^{3.45}) \times 10^{1.607e^{-B^2}} \quad (7)$$

356 For values of particle radius r and an adjustable parameter  $\Theta = 30$ , which controls the  
357 shape of the sub-micron size distributions, the constants A and B are given by equations 8  
358 and 9.

$$A = 4.7(1 + \Theta r)^{-0.017r^{-1.44}} \quad (8)$$

$$B = (0.433 - \log r)/0.43 \quad (9)$$

### 361 *Treatment of emissions from large stacks*

362 As the modelled air mass tracks along a trajectory, the emissions are entered  
 363 independently of any height constraint into the boundary layer, suggesting a possible  
 364 reason for the initially high SO<sub>2</sub> values (c.a. 2.5 times the expected value). Redington and  
 365 Derwent (2002) also reported a similar problem with SO<sub>2</sub> concentrations calculated by  
 366 their NAME model. The highest emissions of SO<sub>2</sub> on the emission maps were attributable  
 367 to coal- and oil-fired power stations, together with other heavy industries (illustrated for the  
 368 UK in Figure S3). Given that major industrial emissions are made via tall chimney stacks  
 369 (100-300 m), there will be times of the day when the emissions are not made into the  
 370 boundary layer but above it. Compared to state-of-the art 3-D models, where the  
 371 emissions can be injected into the relevant model layer, this is a limitation of the boundary-  
 372 layer model.

373 Bieser et al. (2011) calculated the vertical emission profiles of point-source emissions  
 374 over Europe, evaluating an average effective emission height from plume rise calculations  
 375 applied to various meteorological fields, seasons, times of the day and emission stack  
 376 characteristics. In this work, an empirical equation (10) - approximating the findings of  
 377 Bieser et al. (2011) - was derived by re-aggregating the calculated fractional values for the  
 378 binned emission heights.

$$AFV(h) = \begin{cases} 0, & h < 144 \text{ m} \\ 0.45 + \tan^{-1}(1.02 * h - 310.6)/2.49, & 144 \text{ m} < h < 724 \text{ m} \\ 1, & h \geq 724 \text{ m} \end{cases} \quad (10)$$

379 where AFV(h) represents the mixing height (h)-dependent average fractional value of the  
 380 emissions.

381 Using equation 10, the chimney code cuts the SNAP 1 NO<sub>x</sub> and SO<sub>2</sub> emission fluxes  
 382 by the fractional value AFV(h), if (i) the air mass passes over an emission square  
 383 containing a major point source and (ii) the boundary layer height is less than 724 m, when  
 384 it starts to slice the average emission plume.

385 The locations of emitting stacks were identified in the model using positional data  
 386 published by the European Environment Agency's European Pollutant Release and  
 387 Transfer Register (E-PRTR). (<http://prtr.ec.europa.eu/>) In total, 417 UK and 5171  
 388 European NO<sub>x</sub> and SO<sub>2</sub> emitters are accounted for in this way within the model. The  
 389 inclusion of a "chimney code" attempts to overcome the limitation of a single box to

390 describe the boundary layer. As a result, the relatively high NO<sub>x</sub> and SO<sub>2</sub> concentrations  
391 are reduced by 69% and 91% on average respectively relative to the base case of 11.18  
392 ppb and 2.43 ppb without the “chimney code”. Future model enhancements may well  
393 seek to account for the seasonal and daily activity of the power stations according to  
394 expected output.

395 The main local source of SO<sub>2</sub> and NO<sub>x</sub> within the vicinity of the Harwell site is Didcot  
396 power station which is an 1.9 GW coal fired station used to meet peak demand. This is  
397 located 7 km downwind of Harwell for the prevailing south-westerly air masses, and it has  
398 been shown in a past study (Jones and Harrison, 2011) that Didcot power station has  
399 virtually no influence on the measurements at Harwell, and thus the SO<sub>2</sub> and NO<sub>x</sub>  
400 emissions are reduced to zero for Didcot Power station in the model. This conclusion was  
401 drawn from data collected at Harwell from 2001 to 2008 and is thought to be due primarily  
402 to the lofting of the chimney emissions above the air sampled at Harwell.

403

#### 404 **Computation**

405 The model was coded using the FACSIMILE numerical integration package (Curtis  
406 and Sweetenham, 1988). For each species *i* within the air parcel, its concentration within  
407 the boundary-layer  $C_i$  is governed by the differential equation (11)

$$\frac{d}{dt}[C_i] = P_i + \frac{E_i}{H} - L_i[C_i] - \frac{v_g}{H}[C_i] - ([C_i] - [B_i])\frac{1}{H}\frac{dH}{dt} \quad (11)$$

408 The source terms include the local emission rate from pollution sources  $E_i$  and the  
409 production rate of the species from photochemistry  $P_i$ . Similarly, the loss terms include the  
410 loss rate by photochemistry  $L_i C_i$  and dry deposition rate  $\frac{v_g}{H}[C_i]$ . The effect of boundary  
411 layer height changes is represented by the time-dependent variable  $H$ .  $B_i$  is the  
412 concentration of the species in the supra boundary layer. The differential equations were  
413 solved using the variable order GEAR solver in the FACSIMILE software package.

414

#### 415 **Model Validation**

416 The model was used to simulate a wide range of PM concentrations measured at the  
417 Harwell site in southern England (latitude = 51.571°N and longitude = 1.325°W). The  
418 primary test of the model was against daily concentrations of chloride, nitrate and sulphate  
419 collected at the Harwell site as part of the Airborne Particle Concentrations and Numbers  
420 Network (Hayman, 2008). The daily samples were collected using a Partisol 2025 sampler  
421 fitted with a PM<sub>10</sub> inlet. In addition hourly concentrations of NO, NO<sub>x</sub>, CO and O<sub>3</sub> data were  
422 measured using chemiluminescence, IR Absorption and UV absorption respectively. The

423 data are verified and ratified every quarter using the results from independent QA/QC site  
424 audits (see link for more details  
425 [http://www.airquality.co.uk/verification\\_and\\_ratification.php](http://www.airquality.co.uk/verification_and_ratification.php)).

426 Other analytes were taken from other networks offering either a monthly or an hourly  
427 resolution. Monthly measured data was taken from the Acid Gas and Aerosol Network  
428 (AGANET) and the National Ammonia Monitoring Network (NAMN). These are two of the  
429 four components of the UK Eutrophying and Acidifying Atmospheric Pollutants (UKEAP)  
430 network (<http://pollutantdeposition.defra.gov.uk/aganet>). The UKEAP measurements were  
431 carried out using the CEH DELTA (DENuder for Long-Term Atmospheric sampling) system  
432 which is a low-cost diffusion denuder system that was originally developed for long-term  
433 sampling of ammonia and ammonium (Sutton et al., 2001), and which has also been  
434 tested for long-term sampling of acid gases ( $\text{HNO}_3$ , HONO, HCl,  $\text{SO}_2$ ) and aerosols ( $\text{NO}_3^-$   
435  $\text{NO}_2^-$ ,  $\text{Cl}^-$ ,  $\text{SO}_4^{2-}$ ) (Tang et al., 2008). Quality Assurance is maintained through the  
436 implementation of established sampling protocols, and monitoring of laboratory  
437 performance through participation in the EMEP and WMO-GAW inter-comparison  
438 schemes for analytical laboratories. The data quality is assessed using set Quality Control  
439 criteria: a) based on the capture efficiency using two denuders in the DELTA systems and  
440 b) involving the coefficient of variation for ammonia concentrations with the triplicate  
441 ALPHA samplers. Further details of the measurements and verification/ratification  
442 procedures are given in the annual reports to DEFRA (see link [http://www.uk-](http://www.uk-pollutantdeposition.ceh.ac.uk/reports)  
443 [pollutantdeposition.ceh.ac.uk/reports](http://www.uk-pollutantdeposition.ceh.ac.uk/reports)).

444

## 445 **RESULTS**

### 446 **Generalisation of the Patterns Observed in the Daily Back Trajectories**

447 Data from the period 19 March 2007 to 18 May 2007 were used for the validation  
448 capturing a large range of  $\text{PM}_{10}$  values to model. The patterns observed in the measured  
449 daily PM values can be accounted for by how the 24 hourly back trajectories (for the  
450 measurement day) spread across the emission map (see Figure S6). At the start of the  
451 sampling period (19<sup>th</sup> March) an increase – from relatively small concentrations - in the  
452 nitrate and sulphate values - was observed after the third day (Figure 2). This is  
453 accounted for by the air mass trajectories switching their origins from over the North Pole  
454 (passing directly down through Scotland and Northern England to the receptor site on  
455 20/03/2007) to an origin in Eastern Europe on 25<sup>th</sup> March (25/03/2007 in Figure S6). The  
456 air masses continued to originate from eastern Europe up until 2<sup>nd</sup> April (03/04/2007) after  
457 which the starting points of the trajectories move towards the North Sea and then towards

458 the Atlantic off the coast of Republic of Ireland and France between 3<sup>rd</sup> and 14<sup>th</sup> April  
459 (09/04/2007). From 15<sup>th</sup> April to 5<sup>th</sup> May the trajectories start at locations close to the west  
460 and east coast of the UK, crossing over France, Germany and Denmark periodically  
461 (15/04/2007). Then in the final phase of the sampling period 6-19<sup>th</sup> May, the air masses  
462 have their origin firmly in the middle of the Atlantic Ocean (18/05/2007). In general, when  
463 the air mass spends most of its time over the sea, the chloride measurements are high  
464 and the nitrate and sulphate are low (see Figure 2). Conversely, when the air mass  
465 originates over land and passes mainly over land, then the chloride measurements are low  
466 and the nitrate and sulphate measurements are high, consistent with the clustered back  
467 trajectory measurements of Abdalmogith and Harrison (2005). When considering the time  
468 series of predicted and modelled chloride, nitrate and sulphate, the model output  
469 impressively tracks the measured nitrate values. Similarly, the modelled sulphate values  
470 satisfactorily track the measured values but with a high degree of scatter shown by the  
471 plotted hinges. The performance of chloride is not as impressive but is acceptable when  
472 considered in the context of the range of modelled values with nitrate and sulphate.

473

#### 474 **Model Verification and Validation**

475 Table 2 compares the simple statistical values calculated for the gases  $\text{NH}_{3(g)}$ ,  $\text{HNO}_3$ ,  
476  $\text{SO}_2$ ,  $\text{HCl}$ ,  $\text{CO}$ ,  $\text{NO}$ ,  $\text{NO}_2$  and  $\text{O}_3$  and the aerosol components  $\text{NH}_4^+$ ,  $\text{Cl}^-$ ,  $\text{NO}_3^-$ ,  $\text{SO}_4^{2-}$ , for the  
477 period 02/04/2007 to 30/04/2007, across which the average temperature and relative  
478 humidity were 11°C and 72 % respectively. This period corresponds to the monthly  
479 denuder and aerosol filter measurement for April made on the Acid, Gases and Aerosol  
480 Network (AGANET). Considering the core functionality of the enhanced-PTM in  
481 predicting ozone, the model under-predicts  $\text{O}_3$ ,  $\text{NO}$  and  $\text{NO}_2$  by 20%, 64% and 46%  
482 although the ratio of  $\text{NO}_2$  to  $\text{NO}$  is similar for both modelled and measured values.

483 The enhanced model under-predicts mean values of ammonia gas, ammonium, nitric  
484 acid and hydrochloric acid by 12 %, 0 %, 88 % and 96 % respectively. In the original  
485 model, there was an overestimation of sulphur dioxide as also reported by Redington and  
486 Derwent (2002). By using the height dependent emission of  $\text{SO}_2$ , prescribed in the  
487 chimney code, we have brought this prediction down from a mean value of 2.43 ppb to a  
488 mean value of 0.27 ppb. With regards to the particulate matter concentrations, the model  
489 over-predicts the measured value of chloride, nitrate and sulphate by 20 %, 8.1 % and  
490 18% respectively. Although these discrepancies appear large, the model results appear  
491 more reasonable when comparing with the full time series (Figure 2 & 3).

492 The improvement in the capability of the enhanced PTM to model nitrate and  
493 sulphate can be judged from Figure 2 where a comparison with the original model output is  
494 presented. Both original and enhanced modelled values of nitrate and sulphate do indeed  
495 span the range of measured values for the sampling period considered but the original  
496 model fails to account for specific scenarios thus leading to a short-fall in the calculated  
497 nitrate and sulphate values. The original model did not calculate chloride but the  
498 comparison shows that the enhancements made to the model address the general under  
499 prediction of nitrate and sulphate. The original PTM was capable of modelling the more  
500 significant nitrate and sulphate episodes associated with easterly back trajectories but  
501 failed to account for the smaller episodes resulting from westerly trajectories. This led to  
502 sharp increases in nitrate and sulphate when the air masses switched from westerly to  
503 easterly (14/04/2007-15/04/2007). The enhanced model accounts better for the high  
504 values observed during the nitrate episodes, especially the episode between 25<sup>th</sup> and 27<sup>th</sup>  
505 March where the nitrate value reached  $36 \mu\text{g m}^{-3}$ . This episode was initially thought to be  
506 due to the presence of fog, although the meteorology measured at the nearby met-station  
507 of Benson did not indicate this to be the case. However, weather diaries for these three  
508 days record the UK weather as being generally dry by day due to an anticyclonic ridge,  
509 which can be associated with overnight fog. (see link:  
510 <http://www.met.rdg.ac.uk/~brugge/diary2007.html>). The trajectories for this period  
511 originated over central and eastern Europe thus leading to the observed sulphate episode.  
512 The enhanced model also reflected, but over-predicted, later sulphate episodes  
513 (12/04/2007-18/04/2007 and (20/04/2007-24/04/2007). Whereas the original model  
514 represented this episode by a brief spike in the sulphate values, the new model, which is  
515 able to model episodes due to westerly air masses, shows a longer episode better  
516 matching the measured data.

517 A direct comparison of the calculated and measured data is shown in Figure 3 where  
518 the time-series data has been replotted. The poor performance of the model to account  
519 for chloride can be immediately seen by the large fraction of points which are respectively  
520 either above or below the marked 2:1 or 1:2 boundary. Although the general trend is  
521 correct, there is a significant amount of scatter about the fitted and 1:1 line showing that  
522 there is a weakness in the modelling of chloride to be accounted for. The plots for nitrate  
523 and sulphate are much better with the majority of points within the 2:1 and 1:2 boundary.  
524 The over-prediction of sulphate results in a larger than unity gradient for sulphate, and the  
525 less than unity gradient of nitrate suggest the model is still slightly under-estimating the

526 higher values seen during the episodes.

527 Even though some of the higher measured chloride values are under-predicted, the  
528 temporal trends predicted by the model reflect the measured values fairly well as seen in  
529 Figure 2. This gives confidence in the ability of the Gong parameterisation and  
530 ISORROPIA II parameterisation to model the correct magnitude of sea salt, although the  
531 measured value was in general within or just outside of the max/min modelled values.  
532 This large discrepancy may be accounted for by uncertainties in the trajectory values of 10  
533 m wind speed. Good results are obtained for nitrate for which the median daily value was  
534 much closer to the PM value. With regards to sulphate, the PTM was able to model  
535 correctly both high and low sulphate episodes although with a very high scatter of values  
536 as depicted by the max/min point of the plotted hinges. Also, there were periods where  
537 sulphate was significantly over-predicted.

538 Table 3 considers the effect of the model enhancements - measured against the daily  
539 observed PM measured values - using performance metrics calculated separately for the  
540 original and enhanced UK-PTM. The complete 61 day measurement period was  
541 considered for this comparison and the enhanced model improves considerably the  
542 average calculated values for the period. Both nitrate and sulphate were under-predicted  
543 relative to the observed values by 56% using the original model. The enhancements  
544 reduced this discrepancy for nitrate and sulphate to within 1.5% and 3.3% of the measured  
545 mean values and the calculated chloride value was within 13% of the measured value.  
546 Furthermore, improvements in how well the calculated values track with the measured  
547 values are reflected in the values of Spearman's correlation coefficient  $r$  which increase  
548 from approximately 0.5 to 0.83 and 0.65 for nitrate and sulphate respectively. As Figure 3  
549 also indicates, the correlation coefficient of 0.5 for the chloride values shows that the  
550 model does not estimate chloride as well as it calculates nitrate and sulphate.

551 The Root Mean Square Error, RMSE provides information on the short term  
552 performance and has a possible range from 0 to  $+\infty$  (Derwent 2009a). Again, the closer  
553 this value is to zero the better is the short term performance and although fractional values  
554 are not achieved using the enhanced model and we do not better the values of Derwent et  
555 al. (2009b) modelling longer time series measurements at Harwell with a UK-PTM, a  
556 considerable improvement in the short term performance of the PTM can be seen in our  
557 enhanced model. The Index of Agreement, IA, reflects the improvement in performance.  
558 IA is a statistical measure of the correlation of the predicted and measured concentration;  
559 the closer this is to 1 the better the correlation. For nitrate and sulphate an increase in the

560 value of IA is observed from 0.88 and 0.86 to 0.96 and 0.95 respectively. The value of IA  
561 for chloride is also unexpectedly high considering the values of Spearman correlation  
562 coefficient ( $r$ ). As argued by Nath and Patil (2006) the value of  $r$  is often misleading as it  
563 may be unrelated to the size of difference between observed and predicted values, and  
564 that IA is better measure of how two values track each other over a period of time.

565 The improvement in the calculation of nitrate and sulphate is reflected also in the  
566 improved value of the mean bias error MB. The Mean Bias, MB provides information on  
567 the long term performance and has a range between the negative of the mean observed  
568 value to  $+\infty$ . The closer this value is towards zero the better the long term performance.  
569 For both nitrate and sulphate the MB value is reduced to fractional values implying that the  
570 model's long term performance is improved. The fractional MB value for chloride also  
571 indicates that the model's long term performance in calculating chloride is comparable to  
572 that of nitrate and sulphate. Considering the Normalised Mean Bias (NMB) values, if these  
573 lie between -0.2 and 0.2 then the model is acceptable according to the recommendation of  
574 Derwent et al. (2009a). For the case of the nitrate and sulphate values respectively, the  
575 values decrease in magnitude from -0.59 and -0.58 respectively using the original model to  
576 0.05 and -0.07 for the enhanced model (cf the average values of Derwent et al. (2009a) of  
577 0.05 and 0.14 for the whole year ). The NMB value of -0.1 for chloride indicates that the  
578 model's performance is acceptable but far from ideal. This is also reflected by the fraction  
579 of the calculated chloride concentrations FAC2, within a factor of two of the observed  
580 values, being just less than 50 %. For nitrate and sulphate this FAC2 value is 77 % and 81  
581 % respectively. Using the original model the fraction of calculated nitrate and sulphate  
582 values within a factor of 2 of the observed values was 18% and 11% respectively.

583 The contribution of each enhancement can be judged in Table 4. In this, the results  
584 from the enhanced model are compared with the chloride, nitrate and sulphate values  
585 when each enhancement is restored to its original setting. For each case, the decrease in  
586 performance is represented by each percentage. Considering the percentage change in  
587 the arithmetic means, the significance of the enhancements has been ranked from top to  
588 bottom in the table. The most significant enhancement for chloride, nitrate and sulphate is  
589 observed when the replacement of parameterisation of temperature, relative humidity and  
590 the boundary layer height by values modelled by HYSPLIT. This is closely followed by the  
591 enhanced photolysis values for just chloride and nitrate and then by the inclusion of  
592 ISORROPIA II and cloud cover in the model for nitrate. The enhancement of the liquid  
593 phase oxidation of  $\text{SO}_2$  to  $\text{H}_2\text{SO}_4$  in clouds by equation 2, inclusion of stack height  
594 dependent emissions and the improvement in the initial conditions contribute most to the

595 sulphate enhancement. These trends are also observed with the percentage change of  
596 the NMB values and in the context of a limit of acceptability of  $\pm 0.2$ , the largest changes  
597 were seen for sulphate. Similar comparisons were made for FAC2 and  $r^2$  and although the  
598 changes were not as significant, again, the maximum changes were observed for  
599 sulphate.

600 For policymaking decisions, Derwent et al. (2009b) showed that a 30% abatement of  
601 either  $\text{NH}_3$ ,  $\text{NO}_x$  or  $\text{SO}_2$  led to at least 3.5% reduction of either nitrate or sulphate.  
602 Reducing  $\text{NH}_3$  by 30% reduced nitrate and sulphate by 12.2% and 0% respectively  
603 compared to a 14.8% and 2.3% reduction when abating  $\text{NO}_2$  (Derwent et al., 2009b). The  
604 abatement of  $\text{SO}_2$  yielded the highest reduction (of 14.8%) of the contribution of sulphate  
605 to the PM value. The abatement of CO had no effect on the PM contribution from  
606 ammonium, nitrate or sulphate. Likewise, the abatement of VOCs reduced the  
607 contribution to PM from ammonium, nitrate and sulphate by 0 %, 2.1 % and 0.6 %  
608 respectively. Referring to Table 5, our model shows comparable findings. Abating  $\text{NH}_3$  by  
609 30 % reduced nitrate and sulphate by 5.1 % and 0.1 % respectively. Similarly, lowering  
610  $\text{NO}_x$  by 30 % reduced nitrate and sulphate by 17.7 % and 1.9 % respectively. The 30 %  
611 abatement of  $\text{SO}_2$  yielded the highest reduction (by 20.8 %) of the contribution to the PM  
612 value via sulphate and 2.5% of nitrate. For  $\text{NO}_x$  and  $\text{SO}_2$ , our enhanced model predicts a  
613 larger reduction of nitrate and sulphate respectively, compared to Derwent et al. (2009b)  
614 suggesting that our enhancements are potentially accounting for additional sensitivity to  
615 the abatement of these precursors. The model suggests that the abatement of any of  $\text{NH}_3$ ,  
616  $\text{NO}_x$ , or  $\text{SO}_2$  by 30% will lead to a reduction in the sum of  $\text{SO}_4^{2-}$ ,  $\text{NO}_3^-$  and  $\text{Cl}^-$  of between  
617 3.1 % to 8.5 %, with the largest reduction due to  $\text{NO}_x$  abatement.

618

## 619 **SUMMARY**

620 Modifications to the UK Photochemical Trajectory model have been made in order to  
621 make the chemical and meteorological processes more representative of the actual  
622 conditions leading to the composition of the air masses sampled. The principal aim of this  
623 work has been to model values of chloride, nitrate and sulphate over a fixed period of time  
624 where a varied range of hourly nitrate values have been encountered resulting from air  
625 mass trajectories with origins both over sea and continental Europe. Although the full  
626 episodic trends of nitrate have not been totally accounted for by the enhancement, the  
627 nitrate, sulphate and chloride have been modelled far more satisfactorily in comparison to  
628 the original model.

629 When the original and enhanced UK-PTM are evaluated against the criteria  
630 established by Derwent et al. (2009a) for deciding the adequacy of models for policy  
631 relevant queries, we observe a general improvement in the performance metrics. The  
632 largest improvement is seen for the nitrate concentration with the mean bias falling to well  
633 below 0.05 with 77 % of the values lying within a factor of two of the observed values. The  
634 calculations of sulphate had a mean bias of 0.07, and 88 % of the values lay within a factor  
635 of two of the observed values. The calculation of chloride however needs improvement  
636 having a normalised mean bias of -0.1 with 42 % of the calculated values lying within a  
637 factor of two of the observed values. In general, the original model under predicted the  
638 average observed values by 55% and using the enhancements the model calculates  
639 nitrate and sulphate to within 1.5% and 3.3% of the mean measured values. Furthermore,  
640 the enhancements have improved the correlation between the calculated and measured  
641 values reflected by the increase in the Index of Agreement from 0.88 and 0.86 to 0.96 and  
642 0.95 for nitrate and sulphate respectively. Similarly, improvements in the model's ability to  
643 represent the long and short term trends in both nitrate and sulphate have been  
644 demonstrated by the lowering of the values of the normalised mean bias and root mean  
645 square error towards the preferred values of zero. Our model indicates that a 30%  
646 abatement of either NH<sub>3</sub>, NO<sub>x</sub> or SO<sub>2</sub>, will lead to a reduction in the sum of chloride, nitrate  
647 and sulphate of between 3.1 % to 8.5 % (with a corresponding estimated reduction of 1.6 –  
648 3.7% reduction in PM<sub>10</sub>). The largest reduction in this contribution is due to the abatement  
649 of NO<sub>x</sub>.

650

## 651 **ACKNOWLEDGEMENT**

652 The National Centre for Atmospheric Science is funded by the U.K. Natural  
653 Environment Research Council. This work was also supported by the European Union  
654 EUCAARI (Contract Ref. 036833) and EUSAAR (Contract Ref. 026140) research projects,  
655 and by the U.K. Department of Environment, Food and Rural Affairs (Contract Ref.  
656 CPEA28).

657

658

659 **REFERENCES**

660

661 Aas, W., Bruckmann, P., Derwent, R., Poisson, N., Putaud, J.-P., Rouil, L., Vidic, S. and  
662 Karl-Espen Yttri, K.-E., 2007. EMEP Particulate Matter Assessment Report, EMEP/CCC-  
663 Report 8/2007, REF O-7726.

664

665 Abdalmogith, S.S. and Harrison, R.M.,2005. The use of trajectory cluster analysis to  
666 examine the long-range transport of secondary inorganic aerosol in the UK., Atmospheric  
667 Environment, 39, 6686-6695.

668

669 Abdalmogith, S.S., Harrison., R.M. and Derwent, R.G., 2006. Particulate sulphate and  
670 nitrate in Southern England and Northern Ireland during 2002/3 and its formation in a  
671 photochemical trajectory model, Science Total Environment, 368, 769-780.

672

673 AQEG,2005. Particulate Matter in the UK: Summary, Air Quality Expert Group, Defra,  
674 London.

675

676 Atkinson, R., 1997. Gas phase tropospheric chemistry of volatile organic compounds: 1.  
677 Alkanes and alkenes. Journal of Physical and Chemical Reference Data, 26, 215-290.

678

679 Ayers, G.P., 2001. Technical Note: Comment on Regression Analysis of Air Quality Data,  
680 Atmospheric Environment, 35, 2423-2425.

681

682 Baker, J., 2010. A cluster analysis of long range air transport pathways and associated  
683 pollutant concentrations with the UK, Atmospheric Environment, 44, 563-571.

684

685 Beekmann, M., Kerschbaumer, A., Reimer, E., Stern, R. and Moller, D., 2007. PM  
686 measurement campaign HOVERT in the Greater Berlin area: model evaluation with  
687 chemically specified observations for a one year period, Atmospheric Chemistry & Physics,  
688 7, 55–68.

689

690 Bessagnet, B., Menut, L., Curci, G., Hodzic, B., Guillaume, A., Liousse, C., Moukhtar, S.,  
691 Pun, B., Seigneur, C. and Schulz, M., 2009. Regional modeling of carbonaceous aerosols  
692 over Europe - Focus on Secondary Organic Aerosols. Journal of Atmospheric Chemistry,  
693 61, 175–202.

694

695 Bieser, J., Aulinger, A., Matthias, V., Quante, M. and Denier van der Gon, H.A.C., 2011.  
696 Vertical emission profiles for Europe based on plume rise calculations. Environmental  
697 Pollution, 159, 2935-2946.

698

699 Chemel, C., Sokhi, R.S., Yu, Y., Hayman, G.D., Vincent, K.J., Dore, A.J., Tang, Y.S., Prain,  
700 H.D. and Fisher, B.E.A., 2010. Evaluation of a CMAQ simulation at high resolution over  
701 the UK for the calendar year 2003, Atmospheric Environment , 44, 2927-2939.

702

703 Cuvelier, C., Thunis, P., Vautard, R., Amann, M., Bessagnet, B., Bedogni, M., Berkowicz,  
704 R., Brant, J., Brocheton, F., Builtjes, P., Carnavale, C., Coppalle, A., Denby, B., Douros, J.,  
705 Graf, A., Hellmuth, O., Hodzic, A., Honore, C., Jonson, J., Kerschbaumer, A., de Leeuw, F.,  
706 Minguzzi, E., Moussiopoulos, N., Pertot, C., Peuch, V.H., Pirovano, G., Rouil, L., Sauter,  
707 F., Schaap, M., Stern, R., Tarrason, L., Bignati, E., Volta, M., White, L., Wind, P. and  
708 Zuber, A., 2007. CityDelta: A model intercomparison study to explore the impact of  
709 emission reductions in European cities in 2010, Atmospheric Environment, 41, 189-207.

710

711 Curtis, A.R. and Sweetenham, W.P., 1988. FACSIMILE/CHEKMAT Users Manual. AERE  
712 Report R12805. Harwell Laboratory, Oxfordshire, UK.  
713

714 Derwent, D., Fraser, A., Abbott, J., Jenkin, M., Willis, P. and Murrells T., 2009a. Evaluating  
715 the Performance of Air Quality Models, Report to the Department for Environment, Food  
716 and Rural Affairs, Welsh Assembly Government, the Scottish Executive and the  
717 Department of the Environment for Northern Ireland ED48749801 Issue 2.  
718

719 Derwent, R., Witcham, C., Redington, A., Jenkin, M., Stedman, J., Yardley, R. and Hayman,  
720 G., 2009b. Particulate matter at a rural location in southern England during 2006: Model  
721 sensitivities to precursor emissions, *Atmospheric Environment* , 43, 689-696.  
722

723 Derwent R.G., Jenkin M.E., Saunders S.M., Pilling M.J. and Passant N.R., 2005. Multi-  
724 day ozone formation of alkenes and carbonyls investigated with a Master Chemical  
725 Mechanism under European conditions., *Atmospheric Environment* , 39, 627-635.  
726

727 Derwent, R.G., Jenkin, M.E., Saunders, S.M. and Pilling, M.J., 1998. Photochemical  
728 ozone creation potentials for organic compounds in North West Europe calculated with a  
729 Master Chemical Mechanism, *Atmospheric Environment* , 32, 2419-2441.  
730

731 Draxler, R.R. and Hess, G.D., 1998. An overview of the HYSPLIT-4 modelling system for  
732 system for trajectories, dispersion and deposition, *Australian Meteorological Magazine*, 47,  
733 295 -308.  
734

735 EC, 2008. Directive 2008/50/EC of the European Parliament and of the Council of 21 May  
736 2008 on Ambient air quality and cleaner air for Europe. Official Journal of the European  
737 Union, 11.6.2008, L 152/1.  
738

739 Erisman, J.W. and Schaap M., 2004. The need for ammonia abatement with respect to  
740 secondary PM reductions in Europe, *Environmental Pollution*, 129, 159–163.  
741

742 Fountoukis, C. and Nenes, A., 2007. ISORROPIA II: A Computationally Efficient Aerosol  
743 Thermodynamic Equilibrium Model for  $K^+$ ,  $Ca^{2+}$ ,  $Mg^{2+}$ ,  $NH_4^+$ ,  $Na^+$ ,  $SO_4^{2-}$ ,  $NO_3^-$ ,  $Cl^-$ ,  $H_2O$   
744 Aerosols., *Atmospheric Chemistry & Physics*, 7, 4639–4659.  
745

746 Fountoukis, C., Nenes, A., Sullivan, A., Weber, R., VanReken, T., Fischer, M., Matias, E.,  
747 Moya, M. Farmer, D., and Cohen, R., 2009. Thermodynamic characterization of Mexico  
748 City Aerosol during MILAGRO 2006, *Atmospheric Chemistry & Physics*, 9, 2141-2156.  
749

750 Gong, S.L., 2003. A parameterisation of sea-salt aerosol source function for sub- and  
751 super-micron particles, *Global Biogeochemical Cycles*, 17, 1097.  
752

753 Guenther, A., 1997. Seasonal and spatial variations in natural volatile organic compound  
754 emissions. *Applied Ecology* 7, 34-45.  
755

756 Harrison, R.M., Stedman, J. and Derwent, D., 2008. Why are  $PM_{10}$  concentrations in  
757 Europe not falling?, *Atmospheric Environment*, 42, 603-606.  
758

759 Hayman, G., Yardley R., Quincey, P., Butterfield, D., Green, D., Alexander J., Johnson,  
760 P., Tremper A, (2008) NPL REPORT AS 25, CPEA 28: Airborne Particulate Concentrations  
761 and Numbers in the United Kingdom (phase 2) Annual Report - 2007 ISSN 1754-2928.  
762

763 Hayman G.D., Abbott J., Davies, T.J., Thomson C.L., Jenkin M.E., Thetford R. and  
764 Fitzgerald P., 2010. The ozone source-receptor model: a tool for UK ozone policy,  
765 Atmospheric Environment , 44, 4283-4297.  
766

767 Hough, A. M., 1988. The calculation of photolysis rates for use in global tropospheric  
768 modelling studies, United Kingdom Atomic Energy Authority (UKAEA), Harwell Report  
769 AERE H 13259.  
770

771 Jenkin, M.E., Watson, L.A., Utembe, S.R. and Shallcross, D.E., 2008. A Common  
772 Representative Intermediates (CRI) mechanism for VOC degradation. Part 1: Gas phase  
773 mechanism development, Atmospheric Environment , 42, 7185-7195.  
774

775 Jones, A.M. and Harrison, R.M., 2011. Temporal trends in particulate sulphate  
776 concentrations at European sites and relationships to sulphur dioxide, Atmospheric  
777 Environment , 45, 873-882.  
778

779 McMahon, T.A., 1979. Empirical Atmospheric deposition parameters – A survey,  
780 Atmospheric Environment, 3, 571-585.  
781

782 Metcalfe, S.E., Whyatt, J.D., Nicholson, J.P.G., Derwent, R.G. and Heywood, E., 2005.  
783 Issues in model validation: assessing the performance of a regional-scale acid deposition  
784 model using measured and modelled data, Atmospheric Environment , 39, 587-598.  
785

786 Meij de, A., Thunis, P., Bessagnet, B. and Cuvelier, C., 2009. The sensitivity of the  
787 CHIMERE model to emissions reduction scenarios on air quality in Northern Italy,  
788 Atmospheric Environment, 43, 1897-1907.  
789

790 Monteiro, A., Miranda, A.I., Borrego, C., Vautard, R., Ferreira, J. and Perez, A.T., 2007.  
791 Long-term assessment of particulate matter using CHIMERE model, Atmospheric  
792 Environment, 41, 7726-7738.  
793

794 Nath, S. and Patil, R.S., 2006. Prediction of air pollution concentration using an in situ real  
795 time mixing height model, Atmospheric Environment, 40, 3816–3822  
796

797 Nenes, A., Pandis, S.N. and Pilinis, C., 1998a. ISORROPIA: A new thermodynamic  
798 equilibrium model for multiphase multicomponent inorganic aerosols, Aquatic  
799 Geochemistry, 4, 123-152.  
800

801 Nenes, A., Pilinis, C., and Pandis, S.N., 1998b. Continued development and testing of a  
802 new thermodynamic aerosol module for urban and regional air quality models,  
803 Atmospheric Environment, 33, 1553-1560.  
804

805 Passant, N.R. (2002) Speciation of UK Emissions of Non-Methane Volatile Organic  
806 Compounds, AEA Technology, Report No. AEAT/ENV/R/0545 Issue 1  
807

808 PELCOM (2000), Final Report on the Pan-European Land Cover Monitoring project  
809 (PELCOM), funded by the European Commission DGXII (ENV4-CT96-0315).  
810 Report edited by C.A. Mueher and available from  
811 <http://www.geoinformatie.nl/projects/pelcom/public/index.htm>  
812

813 Redington, A.L. and Derwent, R.G., 2002. Calculation of sulphate and nitrate aerosol  
814 concentrations over Europe using a Lagrangian dispersion model, Atmospheric

815 Environment, 36, 4425-4439.  
816  
817 Schaap, M., van Loon, M., ten Brink, H., Dentener, F.J., and Bultjes, P.J.H., 2004.  
818 Secondary inorganic aerosol simulations for Europe with special attention to nitrate,  
819 Atmospheric Chemistry & Physics, 4,857-874  
820  
821 Schaap, M., Timmermans, R.M.A., Sauter, F.J., Roemer, M., Velders, G.J.M., C Boersen,  
822 G.A., Beck, J.P. and Bultjes, P.J.H., 2008. The LOTOS-EUROS model: description,  
823 validation and latest developments, International Journal of Environment and Pollution, 32,  
824 270 290.  
825  
826 Simpson, D., Benedictow, A., Berge, H., Bergstrom, R. Fagerli, H., Gauss, M., Hayman,  
827 G.D., Jenkin, M.W., Jonson, J.E., Nyiri, A, Semeena, V.S, Tsyro, S., Tuovinen, J.P.,  
828 Valdebenito, A., and Wind, P.. 2011. The EMEP MSC-W chemical transport model.  
829 [https://wiki.met.no/\\_media/emep/page1/userguide\\_062011.pdf](https://wiki.met.no/_media/emep/page1/userguide_062011.pdf)  
830  
831 Smith, M.H., Park, P.M., Consterdine, I.E., 1993. Marine aerosol concentrations and  
832 estimated fluxes over the sea. Q.J.R. Meteorol. Soc., 119, 809-824.  
833  
834 Stern, R., Bultjes, P., Schaap, M., Timmermans, R., Vautard, R., Hodzic, A.,  
835 Memmesheimer, M., Feldmann, H., Renner, E., Wolke, R. and Kerschbaumer, A., 2008. A  
836 model inter-comparison study focussing on episodes with elevated PM10 concentrations,  
837 Atmospheric Environment, 42, 4567-4588.  
838  
839 Stohl, A., 1998. Computation, Accuracy and Applications of Trajectories – A Review and  
840 Bibliography, Atmospheric Environment, 32, 947–966.  
841  
842 Sutton, M.A., Tang, Y.S., Miners, B. and Fowler D., 2001. A new diffusion denuder system  
843 for long term, regional monitoring of atmospheric ammonia and ammonium, Water, Air  
844 and Soil Pollution Focus, 1, 145-156.  
845  
846 Tang, Y.S, van Dijk, N., Anderson, M., Simmons, I., Smith, R.I., Armas-Sanchez, E.,  
847 Lawrence, H. and Sutton, M.A., 2008. Monitoring of nitric acid, particulate nitrate and  
848 other species in the UK – 2007, Interim report under the UK Acid Deposition Monitoring  
849 Network to NETCEN/DEFRA.  
850  
851 Thunis, P., Rouil, L., Cuvelier, C., Stern, R., Kerschbaumer, A., Bessagnet, B., Schaap, M.,  
852 Bultjes, P., Tarrason, L. Douros, J., Moussiopoulos, N., Pirovano, G. and Bedogni, M.,  
853 2007. Analysis of model responses to emission-reduction scenarios within the City Delta  
854 project, Atmospheric Environment, 41, 208-220.  
855  
856 Walker, H.L., Derwent, R.G., Donovan, R., and Baker, J., 2009. Photochemical trajectory  
857 modelling of ozone during the summer PUMA campaign in the UK West Midlands, Science  
858 of the Total Environment, 407, 2012-2023.  
859  
860 Watson, L.A., Shallcross, D.E., Utembe, S.R. and Jenkin, M.E., 2008. A Common  
861 Representative Intermediates (cri) mechanism for VOC degradation. Part 2: Gas phase  
862 mechanism reduction, Atmospheric Environment, 42, 7196-7204.  
863  
864 Wesely, M.L. and Hicks, B.B., 2000. A review of the current status of knowledge on dry  
865 deposition, Atmospheric Environment, 34, 2261-2282.  
866

- 867 Whyatt, J.D., Metcalfe, S.E., Nicholson, J., Derwent, R.G., Page, T. and Stedman, J.R.,  
868 2007. Regional scale modelling of particulate matter in the UK, source attribution and an  
869 assessment of uncertainties, *Atmospheric Environment*, 41, 3315-3327.  
870
- 871 Yin, J. and Harrison, R.M., 2008. Pragmatic mass closure study for PM<sub>1.0</sub>, PM<sub>2.5</sub> and PM<sub>10</sub>  
872 at roadside, urban background and rural sites, *Atmospheric Environment*, 42, 980-988.

873 **TABLES LEGENDS**

874 Table 1. Summary of changes made to the UK-Photochemical Trajectory Model.

875  
876 Table 2. Simple statistics calculated using modeled and measured concentrations  
877 collected over the period from 02/04/2007 to 30/04/2007. Mean temperature  
878  $284.3 \pm 2.3\text{K}$  and relative humidity of  $71.8 \pm 6.7\%$ . [\* Values represent the  
879 measured monthly value only. \*\* The  $\text{O}_3$  values represent the period when  
880 measured values were available, from 26/04/2007 to 19/05/2007.]

881  
882 Table 3. Model performance metrics for the period from 19/03/2007 to 19/05/2007 using  
883 full days data. [N = number of complete pairs of measured and calculated  
884 values; MB = mean bias ( $\mu\text{g}/\text{m}^3$ ); NMB = Normalised mean bias; MGE = mean  
885 gross error; NMGE = normalised mean gross error; FAC2 = A count fraction of  
886 points within 0.5 and 2 times the observation; RMSE = root mean square error  
887 ( $\mu\text{g}/\text{m}^3$ ); r = Spearman's correlation;  $r^2$  = correlation coefficient; and IA = Index  
888 of Agreement.]

889  
890 Table 4. Observed changes in values of the Performance Metrics when each  
891 enhancement in the model is restored to its original setting.

892  
893 Table 5. Change of calculated species concentrations (%) resulting from precursor  
894 abatement (by 30%) on the calculated chloride, nitrate and sulphate  
895 concentrations. A comparison is made with the study of Derwent et al. (2009) –  
896 abatement figures shown in italics.

897  
898  
899 **FIGURE LEGENDS**

900 Figure 1. Boundaries separating the Northern, Eastern, Southern, Western and Central  
901 Regions of Europe. Initial concentrations are specified for each region and are  
902 used as initial conditions in each calculation depending on which region the  
903 trajectory starts.

904  
905 Figure 2. Comparison between calculated and measured  $\text{PM}_{10}$  chloride, nitrate and  
906 sulphate. Measurements (black line) were made with a Rupprecht and  
907 Patashnick Partisol 2025 sampler with  $\text{PM}_{10}$  sampling inlet. The calculated data  
908 is depicted by the blue whisker plots derived from the statistics of each group of  
909 24 hourly calculated values. The middle horizontal line represents the median;  
910 the two hinges represent the first and third quartile; and the two whiskers  
911 represent the maximum and minimum values. Also included are the results  
912 shown by the brown line from the initial PTM model. (Referring to Figure 1, the  
913 coloured ribbon at the bottom of each plot shows the zone from which the  
914 trajectory used in the calculation started.)

915  
916 Figure 3. Comparison between calculated and measured  $\text{PM}_{10}$  chloride, nitrate and  
917 sulphate. Measurements made with a Rupprecht and Patashnick Partisol 2025  
918 sampler with  $\text{PM}_{10}$  sampling inlet. The data is fitted using the Reduced Major  
919 Axis method (Ayers, 2001), indicated by the solid black line and equation. Also  
920 included on these correlation plots is the ideal case of a 1:1 correlation marked  
921 out by the blue line and the boundaries where the calculated values are twice or  
922 half the value of the measured values (dashed lines).

923  
924

**Table 1. Summary of changes made to the UK-Photochemical Trajectory Model.**

	<b>Enhancement of</b>	<b>TO</b>	<b>FROM</b>
<b>Emissions</b>	Continental VOC/NOx/CO/SO2/ Biogenics/NH3	EMEP, base year 2005 (50×50 km)	CORINAIR, base year 1985 (150×150 km)
	United Kingdom VOC/NOx/CO/SO2/ Biogenics/NH3	NAEI, base year 2005, (10×10 km)	CORINAIR, base year 1985 (10×10 km)
	Sea Salt flux	Gong (2003) parameterisation	None present
	Boundary layer / free troposphere injection	B.L. height determines input of SO <sub>2</sub> and NO <sub>x</sub> .	None present
	Initial Conditions	Dependent on initial lat/long position being in either a N/E/S/W or Central Region.	Westerly Clean conditions for all trajectories
	<b>Chemical Mechanism</b>	Gas phase	cri-v02
Aqueous phase		ISORROPIA II	None present
Aqueous oxidation of SO <sub>2</sub> ,		Schaap et al. (2004)	None present
Photolysis Rates		Dependent of lat/long, cloud cover and surface.	Based on a parameterisation.
Gaseous dry deposition Rates		Dependent on surface (land/sea)	Fixed values
NO <sub>2</sub> & SO <sub>2</sub> wet deposition Rates		McMahon et al. (1979) parameterisation	None Present
PM deposition rates	Smith et al. (1993) parameterisation	None present	
<b>Back Trajectory Calculation</b>	Lat/Long	Calculated using HYSPLIT	Calculated using BADC
	Mixing Depth	Calculated using HYSPLIT	Saw tooth fn
	Temperature	Calculated using HYSPLIT	Sinusoidal fn
	RH	Calculated using HYSPLIT	Sinusoidal fn
	Cloud Cover	Calculated using HYSPLIT	None present
	U10	Calculated using HYSPLIT	None present
	Rain (YY/MM/DD/HH/MM)	Calculated using HYSPLIT	None present

925  
926  
927  
928  
929  
930  
931  
932  
933

**Table 2. Simple statistics calculated using modeled and measured concentrations collected over the period from 02/04/2007 to 30/04/2007. Mean temperature 284.3 ± 2.3K and relative humidity of 71.8 ± 6.7 %. [\* Values represent the measured monthly value only. \*\* The O<sub>3</sub> values represent the period when measured values were available, from 26/04/2007 to 19/05/2007].**

<b>Const- ituent</b>	Unit	<b>Field Values</b>					<b>PTM Values</b>				
		<i>Min.</i>	<i>Lower quartile</i>	<b>Geo. Mean</b>	<i>Upper quartile</i>	<i>Max.</i>	<i>Min.</i>	<i>Lower quartile</i>	<b>Geo. Mean</b>	<i>Upper quartile</i>	<i>Max.</i>
<b>NH<sub>3(g)</sub></b>	ppb	-	-	6.95	-	-	0.14	3.95	<b>6.11</b>	9.8	22.1
<b>NH<sub>4</sub><sup>+</sup></b>	μg/m <sup>3</sup>	-	-	2.80	-	-	0	0	<b>2.80</b>	5.05	16.9
<b>HNO<sub>3</sub></b>	ppb	-	-	0.59	-	-	0	0.02	<b>0.07</b>	0.28	2.3
<b>SO<sub>2</sub></b>	ppb	-	-	0.99	-	-	0.02	0.12	<b>0.27</b>	0.63	15.9
<b>HCl</b>	ppb	-	-	0.26	-	-	0	0	<b>0.01</b>	0.04	0.99
<b>Cl<sup>-</sup></b>	μg/m <sup>3</sup>	0.13	0.26	<b>0.56</b>	1.10	3.40	0	0.43	<b>0.67</b>	1.42	4.16
<b>NO<sub>3</sub><sup>-</sup></b>	μg/m <sup>3</sup>	2.17	4.56	<b>6.89</b>	10.7	16.4	0.05	4.62	<b>7.45</b>	13.9	35.7
<b>SO<sub>4</sub><sup>2-</sup></b>	μg/m <sup>3</sup>	1.21	2.42	<b>3.62</b>	5.33	9.92	0.48	1.59	<b>4.27</b>	9.39	67.8
<b>CO</b>	ppb	-	-	-	-	-	123.6	150	<b>177.1</b>	200.8	528.5
<b>NO</b>	ppb	0.00	0.00	<b>1.20</b>	2.20	18.8	0.0	0.03	<b>0.43</b>	2.64	115.0
<b>NO<sub>2</sub></b>	ppb	0.00	3.67	<b>7.03</b>	9.98	37.1	0.47	2.46	<b>3.78</b>	5.93	20.2
<b>O<sub>3</sub><sup>**</sup></b>	ppb	7.6	24.4	<b>28.7</b>	36.7	62.1	0	15.8	<b>23.0</b>	28.4	46.3

934

935  
 936  
 937  
 938  
 939  
 940  
 941  
 942

**Table 3. Model performance metrics for the period from 19/03/2007 to 19/05/2007 using full days data. [N = number of complete pairs of measured and calculated values; MB = mean bias ( $\mu\text{g}/\text{m}^3$ ); NMB = Normalised mean bias; MGE = mean gross error; NMGE = normalised mean gross error; FAC2 = A count fraction of points within 0.5 and 2 times the observation; RMSE = root mean square error ( $\mu\text{g}/\text{m}^3$ ); r = Spearman's correlation coefficient; and IA = Index of Agreement.]**

	<i>Chloride</i>	<i>Nitrate</i>	<i>Sulphate</i>
Observed Values			
<i>Arithmetic Mean</i>	1.10	6.75	3.90
<i>St dev</i>	1.02	6.23	2.60
Original Model Values			
<i>Arithmetic Mean</i>	-	2.96	1.73
<i>St dev</i>	-	4.99	4.11
<i>N</i>		58	58
<i>MB</i>	-	-3.93	-2.24
<i>MGE</i>	-	5.10	3.33
<b><i>NMB</i></b>	-	<b>-0.59</b>	<b>-0.58</b>
<i>NMGE</i>	-	0.76	0.86
<i>RMSE</i>	-	6.80	4.43
<b><i>FAC2</i></b>		<b>0.18</b>	<b>0.11</b>
<i>r (Spearman)</i>	-	0.57	0.55
<i>IoA</i>	-	0.88	0.86
Enhanced Model Values			
<i>Arithmetic Mean</i>	0.96	6.85	4.03
<i>St dev</i>	0.52	5.10	3.33
<i>N</i>	57	57	57
<i>MB</i>	-0.11	0.32	0.28
<i>MGE</i>	0.78	2.47	1.82
<b><i>NMB</i></b>	<b>-0.10</b>	<b>0.05</b>	<b>0.07</b>
<i>NMGE</i>	0.71	0.36	0.47
<i>RMSE</i>	1.06	3.94	2.51
<b><i>FAC2</i></b>	<b>0.42</b>	<b>0.77</b>	<b>0.81</b>
<i>r (Spearman)</i>	0.27	0.83	0.65
<i>IA</i>	0.9	0.96	0.95

943

944 **Table 4. Observed changes in values of the Performance Metrics when each enhancement**  
 945 **in the model is restored to its original setting.**  
 946

<i>Enhanced Model Values minus...</i>	$\Delta$ (Arithmetic Mean)			$\Delta$ NMB		
	<i>Cl<sup>-</sup></i>	<i>NO<sub>3</sub><sup>-</sup></i>	<i>SO<sub>4</sub><sup>2-</sup></i>	<i>Cl<sup>-</sup></i>	<i>NO<sub>3</sub><sup>-</sup></i>	<i>SO<sub>4</sub><sup>2-</sup></i>
<i>HYSPLIT temp, RH, BLH values</i>	14%	10.0%	-8.2%	-0.08	-0.18	0.00
<i>Enhanced photolysis rates</i>	-7.4%	-17%	-0.5%	0.15	0.12	-0.09
<i>ISORROPIA II</i>	-	8.0%	0.9%	0.11	0.09	0.01
<i>Aqueous oxidation of SO<sub>2</sub>,</i>	2.1%	2.7%	-30%	0.01	0.03	-0.33
<i>Trajectory dependent initial conditions</i>	4.3%	-0.3%	-26%	-0.02	-0.01	0.22
<i>NO<sub>2</sub> and SO<sub>2</sub> Stack height dependent emissions</i>	-2.1%	-1.9%	14%	0.03	0.00	-0.29
<i>Cloud cover dependent photolysis rates (sunny day scenario)</i>	-1.1%	6.4%	0.9%	-0.01	0.07	0.01

947

948

949

950 **Table 5. Change of calculated species concentrations (%) resulting from precursor**  
 951 **abatement (by 30%) on the calculated chloride, nitrate and sulphate concentrations. A**  
 952 **comparison is made with the study of abatement figures shown in italics.**  
 953

Precursor Abated	<i>Chloride</i>	<i>Nitrate</i>	<i>Sulphate</i>	$\Sigma$ (chloride + nitrate + sulphate)	<i>PM<sub>10</sub></i>
<i>NH3</i>	-2.2	-5.1 (-12.2)	0.1 (0)	-3.1	-1.6
<i>NOx</i>	-0.6	-17.7 (-14.8)	1.9 (2.3)	-8.5	-3.7
<i>SO2</i>	0.8	2.5 (3.5)	-20.8 (-14.8)	-6.1	-2.3

954

955

956

957

958

959

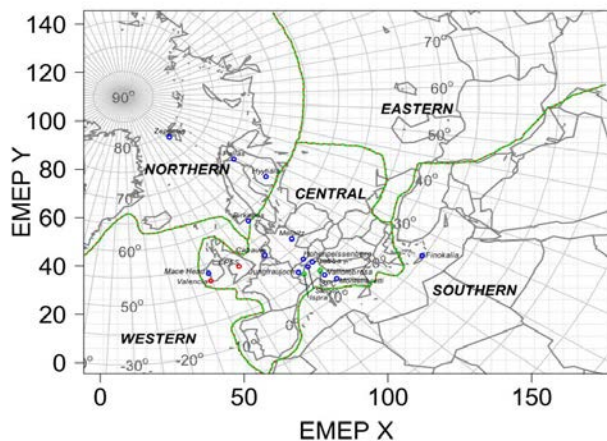


**Figure 1. Boundaries separating the Northern, Eastern, Southern, Western and Central Regions of Europe. Initial concentrations are specified for each region and are used as initial conditions in each calculation depending on which region the trajectory starts.**

960  
961

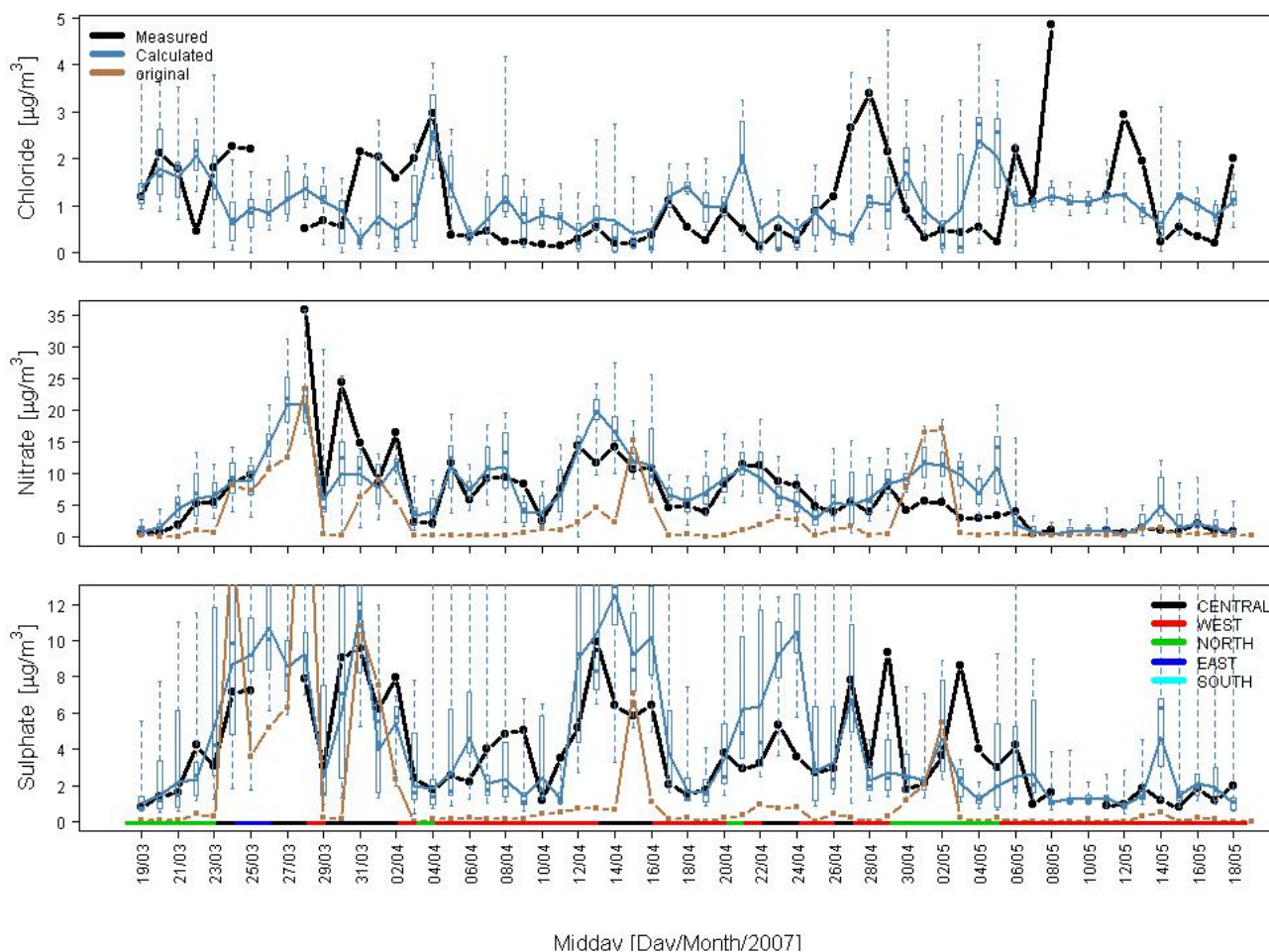


**Figure 2. Comparison between calculated and measured PM<sub>10</sub> chloride, nitrate and sulphate. Measurements (black line) were made with a Rupprecht and Patashnick Partisol 2025 sampler with PM<sub>10</sub> sampling inlet. The calculated data is depicted by the blue whisker plots derived from the statistics of each group of 24 hourly calculated values. The middle horizontal line represents the median; the two hinges represent the first and third quartile; and the two whiskers represent the maximum and minimum values. Also included are the results shown by the brown line from the initial PTM model. (Referring to Figure 1, the coloured ribbon at the bottom of each plot shows the zone from which the trajectory used in the calculation started.)**

962

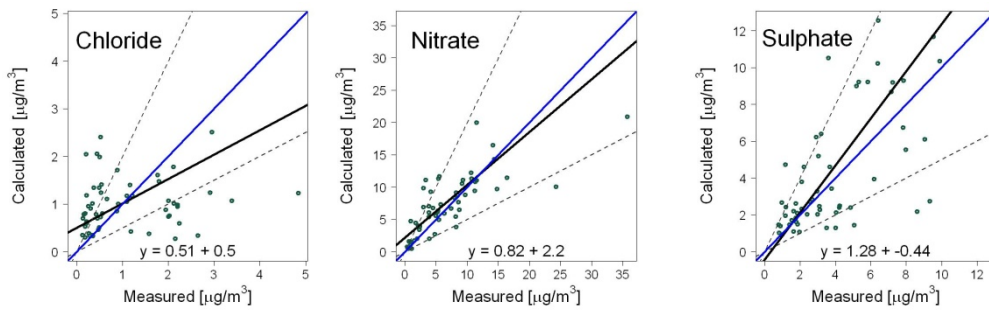


**Figure 3. Comparison between calculated and measured  $\text{PM}_{10}$  chloride, nitrate and sulphate. Measurements made with a Rupprecht and Patashnick Partisol 2025 sampler with  $\text{PM}_{10}$  sampling inlet. The data is fitted using the Reduced Major Axis method (Ayers, 2001), indicated by the solid black line and equation. Also included on these correlation plots is the ideal case of a 1:1 correlation marked out by the blue line and the boundaries where the calculated values are twice or half the value of the measured values (dashed lines).**

963

964